Towards a physical interpretation of the entropic lattice Boltzmann method

Orestis Malaspinas* and Michel Deville†
École Polytechnique Fédérale de Lausanne, 1015 Lausanne, Switzerland

Bastien Chopard‡
University of Geneva, 1211 Geneva, Switzerland

(Received 6 August 2008; published 31 December 2008)

The entropic lattice Boltzmann method (ELBM) is one among several different versions of the lattice Boltzmann method for the simulation of hydrodynamics. The collision term of the ELBM is characterized by a nonincreasing H function, guaranteed by a variable relaxation time. We propose here an analysis of the ELBM using the Chapman-Enskog expansion. We show that it can be interpreted as some kind of subgrid model, where viscosity correction scales like the strain rate tensor. We confirm our analytical results by the numerical computations of the relaxation time modifications on the two-dimensional dipole-wall interaction benchmark.

DOI: 10.1103/PhysRevE.78.066705 PACS number(s): 47.11.−j, 05.20.Dd

I. INTRODUCTION

The lattice Boltzmann method (LBM) has become an established tool in the domain of computational fluid dynamics. It simulates the evolution of macroscopic quantities (such as pressure and velocity) through mesoscopic processes of collision and streaming of idealized particles moving on a lattice with discrete velocities [1].

The most widely used collision operator that allows the recovery of the weakly compressible Navier-Stokes (NS) equations is the so-called lattice Bhatnagar-Gross-Krook model (LBGK). This model corresponds to a single relaxation time process towards a prescribed equilibrium distribution (discrete Maxwellian) as proposed by [2] in the case of the continuous Boltzmann equation. The value of the relaxation time is directly related to the viscosity of the modeled fluid.

Although quite successful, the LBGK model may lack of accuracy and may suffer from numerical instability when the lattice is not fine enough. A lot of research has been conducted to improve the situation ([3–5] among others). We want here to focus on the entropic LBM (ELBM) models [6,7].

The ELBM differs from LBGK by two major aspects. First, the equilibrium is not anymore a discretization of the Maxwell-Boltzmann equilibrium distribution function but, rather, the extremum of a discretized H function under the constraint of mass and momentum conservation. Second, the relaxation time is modified in order to achieve unconditional stability by imposing the condition of nonincreasing H function after the collision.

The goal of this paper is to study in detail how this relaxation time is changing as a function of the flow properties and then to propose a macroscopic interpretation of these changes in terms of a subgrid model.

*orestis.malaspinas@epfl.ch
†michel.deville@epfl.ch
‡bastien.chopard@cui.unige.ch

The paper is organized as follows. In Sec. II we briefly recall the main concepts of the ELBM. In Sec. III we present an analytical expression for the relaxation time as a function of the model variables. An approximation of this expression shows that the relaxation time departs from its bare value by a quantity which scales like the strain rate tensor. In Sec. IV we validate our analytical approximation with respect to the full ELBM. Also, we consider a quantitative comparison of ELBM and LBGK, for the dipole-wall collision benchmark (see [8]). Finally, in Sec. V we present our conclusions.

II. ENTROPIC LATTICE BOLTZMANN METHOD

We now briefly describe the ELBM in order to introduce the concepts and notations used in the following sections. For further information the reader should refer to [6,7].

The ELBM evolution equation reads (in lattice units where the mesh size $\Delta x=1$ and the time step $\Delta t=1$)

$$f_i(\boldsymbol{x}+\boldsymbol{c}_i,t+1)=f_i(\boldsymbol{x},t)+\omega_0\frac{\alpha}{2}[f_i^{eq}(\boldsymbol{x},t)-f_i(\boldsymbol{x},t)], \quad (1)$$

where the f_i, for $i=0,\ldots,q-1$, are the density distribution functions corresponding to the q lattice speeds $\boldsymbol{c}_i$ and f_i^{eq} is the equilibrium distribution function. The quantity $\omega=\omega_0\alpha/2$ is the relaxation frequency. The corresponding relaxation time is then simply $\tau=1/\omega$. The bare relaxation frequency ω_0 is related to the viscosity of the fluid and α is the correction that ensures the unconditional stability of the scheme (see below for more details). Note that the LBGK model also obeys Eq. (1) but with $\alpha=2$ and a specific expression of f^{eq}.

The equilibrium distribution function of the ELBM is defined as the extremum of the following discretized H function:

$$H(\boldsymbol{f})=\sum_{i=0}^{q-1}f_i\ln\left(\frac{f_i}{w_i}\right), \quad \boldsymbol{f}=\{f_i\}_{i=0}^{q-1}, \quad (2)$$

where the w_i are the weights associated with each lattice direction. The extremum of H is calculated under the con-

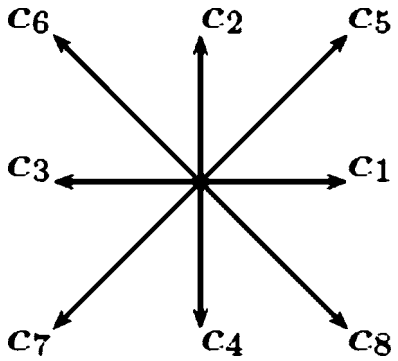

FIG. 1. Velocities $\boldsymbol{c}_i$ connecting a lattice site to its eight neighbors on a D2Q9 lattice. The vector $\boldsymbol{c}_0=0$ is additionally introduced to describe a rest particle population.

straint of mass and momentum conservation (we consider only the athermal case), namely

$$\rho = \sum_{i=0}^{q-1} f_i = \sum_{i=0}^{q-1} f_i^{eq}, \quad \rho \boldsymbol{u} = \sum_{i=0}^{q-1} \boldsymbol{c}_i f_i = \sum_{i=0}^{q-1} \boldsymbol{c}_i f_i^{eq}. \tag{3}$$

The extremalization of Eq. (2) does not have an analytical solution in general, but for the D1Q3 lattice (one dimension and three velocities) and its tensorial products, the D2Q9 and the D3Q27 (see Fig. 1), the expression for f_i^{eq} reads (see [9])

$$f_i^{eq} = w_i \rho \prod_{\gamma=1}^{d} \left\{ \left(2 - \sqrt{1+\frac{u_\gamma^2}{c_s^2}}\right) \left[\frac{\frac{2u_\gamma}{\sqrt{3}c_s} + \sqrt{1+\frac{u_\gamma^2}{c_s^2}}}{1-\frac{u_\gamma}{\sqrt{3}c_s}} \right]^{c_{i\gamma}/(\sqrt{3}c_s)} \right\}, \tag{4}$$

where $c_s=1/\sqrt{3}$ is the speed of sound and d the physical dimension.

The second order moment $\Pi_{\gamma\delta}^{(0)}$ of f_i^{eq} is the nondissipative part of the momemtum tensor and reads

$$\Pi_{\gamma\delta}^{(0)} = \sum_{i=0}^{q-1} c_{i\gamma} c_{i\delta} f_i^{eq} = c_s^2 \rho \delta_{\gamma\delta} + \rho u_\gamma u_\delta + O(\mathrm{Ma}^4), \tag{5}$$

where $\delta_{\gamma\delta}$ is the Kronecker symbol and $\mathrm{Ma}=\|\boldsymbol{u}\|/c_s$ is the Mach number.

Once we have f_i^{eq} we still have to compute α to be able to evaluate the collision operator. It is defined as the solution of [7]

$$H(\boldsymbol{f}) = H(\boldsymbol{f} - \alpha \boldsymbol{f}^{neq}), \tag{6}$$

which represents the maximum H-function variation due to a collision. In this equation we have defined $\boldsymbol{f}^{neq}=\boldsymbol{f}-\boldsymbol{f}^{eq}$.

The above ELBM procedure (computing the equilibrium distribution function and α) allows us to simulate the weakly compressible Navier-Stokes equation up to $O(\mathrm{Ma}^3)$ accuracy [compared to $O(\mathrm{Ma}^2)$ for the LBGK model] and with unconditional stability.

Note that Eq. (6) has to be solved numerically, typically with a Newton-Raphson method. This operation is computationally expensive and, therefore, some optimization techniques have been proposed in [10,11].

III. ELBM AS A SUBGRID MODEL

In this section we derive an analyical approximation for the value of α. We then show that, to first order in Ma, α departs from the value 2 by a quantity containing the strain rate tensor components. Furthermore, this expression scales as the time step Δt, thus revealing a subgrid correction.

The motivation to assume that $\alpha \approx 2$ is that a Chapman-Enskog (CE) expansion (see for instance, [12]) of Eq. (1) shows that the kinematic viscosity ν reads

$$\nu = c_s^2 \left(\frac{2}{\omega_0 \alpha} - \frac{1}{2} \right). \tag{7}$$

Numerical experiments show that the results obtained using the ELBM or the LBGK are quite similar in well-resolved lattices. Thus α must be close to 2. This observation will be mathematically confirmed in Eq. (13) below.

Let us then rewrite α as

$$\alpha = 2 + \beta, \quad |\beta| \ll 1. \tag{8}$$

We can expand Eq. (7) to first order in β,

$$\nu = \nu_0 - \frac{c_s^2}{2\omega_0}\beta + O(\beta^2), \tag{9}$$

where $\nu_0=c_s^2(1/\omega_0-1/2)$ is the bare kinematic viscosity. We see that ν is an effective kinematic viscosity made by the fluid viscosity plus an extra term related to the ELBM. We want to compute this last contribution in order to understand its physical meaning.

Therefore let us evaluate α through Eq. (6). Rewriting $\boldsymbol{f}=\boldsymbol{f}^{eq}+\boldsymbol{f}^{neq}$ and remembering that according to the CE expansion $\boldsymbol{f}^{eq} \sim O(1)$ and $\boldsymbol{f}^{neq} \sim O(\mathrm{Kn})$ (Kn is the Knudsen number) one can expand the right-hand side (rhs) of Eq. (6) around $\boldsymbol{f}^{eq}$ up to $O(\mathrm{Kn}^3)$ [the $O(\mathrm{Kn})$ and $O(\mathrm{Kn}^2)$ terms give the trivial solutions $\alpha=0$ and $\alpha=2$] and one gets (this result is also found in [10])

$$-\frac{\alpha^2}{6}\sum_{i=0}^{q-1}\frac{f_i^{neq3}}{f_i^{eq2}} + \alpha\left(-\frac{1}{2}\sum_{i=0}^{q-1}\frac{f_i^{neq2}}{f_i^{eq}} + \frac{1}{2}\sum_{i=0}^{q-1}\frac{f_i^{neq3}}{f_i^{eq2}}\right) + \underbrace{\sum_{i=0}^{q-1} f_i^{neq} \ln\left(\frac{f_i^{eq}}{w_i}\right)}_{=0} + \sum_{i=0}^{q-1}\frac{f_i^{neq2}}{f_i^{eq}} - \frac{1}{2}\sum_{i=0}^{q-1}\frac{f_i^{neq3}}{f_i^{eq2}} + O(f_i^{neq4}) = 0. \tag{10}$$

We easily see that the term proportional to $\ln(f_i^{eq}/w_i)$ is null by replacing f_i^{eq} according to Eq. (4) and by remembering that the zeroth and the first moments of f_i^{neq} are identically zero.

We are left with the following equation to solve for α:

$$-\frac{C}{6}\alpha^2+\frac{\alpha}{2}(-B+C)+B-\frac{1}{2}C=0, \tag{11}$$

where B and C are defined as

$$B\equiv\sum_{i=0}^{q-1}\frac{f_i^{neq2}}{f_i^{eq}},\quad C\equiv\sum_{i=0}^{q-1}\frac{f_i^{neq3}}{f_i^{eq2}}. \tag{12}$$

In what follows we need to discuss the order of magnitude of different terms. We have two nondimensional numbers involved in the distribution functions, namely the Knudsen and the Mach numbers. These numbers are related by the following relation Kn=Ma/Re, where Re is the Reynolds number. Therefore if we assume that Re>1, we can safely replace the Kn number by Ma in what precedes. This means that $B\sim O(\mathrm{Ma}^2)$ and $C\sim O(\mathrm{Ma}^3)$. Then, solving the quadratic Eq. (11) and keeping only the physically relevant solution for α_+ we find

$$\alpha_+=\frac{3}{2}-\frac{3}{2}\frac{B}{C}+\frac{1}{2C}\sqrt{-3C^2+6BC+9B^2}=2-\frac{C}{3B}+O(\mathrm{Ma}^2), \tag{13}$$

where in the first equality we kept only the "+" part because α_- is nonphysical in the low Mach number limit (scales like 1/Ma) and in the second line we expanded the square root around $9B^2$ up to first order in the Mach number. We now want to evaluate $\beta=-C/(3B)$, the deviation from 2 (i.e., from the LBGK collision). Therefore we replace f_i^{eq} by its value [see Eq. (4)] and expand the fraction to first order in the Mach numbers. We find

$$\beta=-\frac{\Sigma_{i=0}^{q-1}f_i^{neq3}/w_i^2}{3\rho\Sigma_{i=0}^{q-1}f_i^{neq2}/w_i}. \tag{14}$$

To continue the evaluation of β we need an expression for f_i^{neq}. We will approximate its value by the first order term in the CE expansion $f_i^{(1)}$ (see [12,13] for details):

$$f_i^{(1)}=-w_i\Delta t\frac{\rho}{\omega c_s^2}\boldsymbol{Q}_i{:}\boldsymbol{\nabla u}=-w_i\Delta t\frac{\rho}{\omega c_s^2}\boldsymbol{Q}_i{:}\boldsymbol{S} \tag{15}$$

$$=\Delta t\frac{w_i}{2c_s^4}\boldsymbol{Q}_i{:}\boldsymbol{\Pi}^{(1)}, \tag{16}$$

where $Q_{i\alpha\beta}=c_{i\alpha}c_{i\beta}-c_s^2\delta_{\alpha\beta}$, Δt is the time step, and

$$\boldsymbol{S}=\frac{1}{2}[\boldsymbol{\nabla u}+(\boldsymbol{\nabla u})^{\mathrm{T}}],\quad \boldsymbol{\Pi}^{(1)}=\sum_{i=0}^{q-1}\boldsymbol{c}_i\boldsymbol{c}_i f_i-\boldsymbol{\Pi}^{(0)}, \tag{17}$$

and

$$\boldsymbol{\Pi}^{(1)}=-\frac{2c_s^2\rho}{\omega}\boldsymbol{S}.$$

Replacing this relation in Eq. (14) one gets

$$\beta=-\frac{\Delta t}{3\rho c_s^4}\frac{\Sigma_{i=0}^{q-1}w_i(\boldsymbol{Q}_i{:}\boldsymbol{\Pi}^{(1)})^3}{\Sigma_{i=0}^{q-1}w_i(\boldsymbol{Q}_i{:}\boldsymbol{\Pi}^{(1)})^2}. \tag{18}$$

We are now left with the evaluation of the two sums. Let us start with the denominator

$$\begin{aligned}\sum_{i=0}^{q-1}w_i(\boldsymbol{Q}_i{:}\boldsymbol{\Pi}^{(1)})^2&=\Pi_{\varepsilon\zeta}^{(1)}\Pi_{\gamma\delta}^{(1)}\sum_{i=0}^{q-1}w_i(c_{i\varepsilon}c_{i\zeta}-c_s^2\delta_{\varepsilon\zeta})\\&\quad\times(c_{i\gamma}c_{i\delta}-c_s^2\delta_{\gamma\delta})\\&=c_s^4\Pi_{\varepsilon\zeta}^{(1)}\Pi_{\gamma\delta}^{(1)}(\delta_{\varepsilon\gamma}\delta_{\zeta\delta}+\delta_{\varepsilon\delta}\delta_{\zeta\gamma})\\&=2c_s^4\Pi_{\gamma\delta}^{(1)}\Pi_{\gamma\delta}^{(1)},\end{aligned} \tag{19}$$

where between the first and the second step we used the lattice isotropy properties $\Sigma_i w_i c_{i\varepsilon}c_{i\zeta}c_{i\gamma}c_{i\delta}=c_s^4(\delta_{\varepsilon\zeta}\delta_{\gamma\delta}+\delta_{\varepsilon\delta}\delta_{\gamma\zeta}+\delta_{\varepsilon\gamma}\delta_{\zeta\delta})$ and the summation convention over repeated greek indices. We can now evaluate the sum in the numerator of Eq. (18),

$$\begin{aligned}\sum_{i=0}^{q-1}w_i(\boldsymbol{Q}_i{:}\boldsymbol{\Pi}^{(1)})^3&=\Pi_{\theta\kappa}^{(1)}\Pi_{\gamma\delta}^{(1)}\Pi_{\varepsilon\zeta}^{(1)}\sum_{i=0}^{q-1}w_i(c_{i\theta}c_{i\kappa}-c_s^2\delta_{\theta\kappa})\\&\quad\times(c_{i\gamma}c_{i\delta}-c_s^2\delta_{\gamma\delta})(c_{i\varepsilon}c_{i\zeta}-c_s^2\delta_{\varepsilon\zeta})\\&=-c_s^6\Pi_{\gamma\gamma}(6\Pi_{\theta\kappa}^{(1)}+\Pi_{\theta\theta}\Pi_{\kappa\kappa})\\&\quad+K_{\theta\kappa\gamma\delta\varepsilon\zeta}\Pi_{\theta\kappa}^{(1)}\Pi_{\gamma\delta}^{(1)}\Pi_{\varepsilon\zeta}^{(1)},\end{aligned} \tag{20}$$

where $K_{\theta\kappa\gamma\delta\varepsilon\zeta}=\Sigma_{i=0}^{q-1}w_i c_{i\theta}c_{i\kappa}c_{i\gamma}c_{i\delta}c_{i\varepsilon}c_{i\zeta}$. As before the step between the first and the second equation is performed using the isotropy properties of the lattice; but this time we see that we are left with a sixth order tensor. The lattices used to recover the NS equations do not require the sixth order isotropy property (only up to order four is needed). The D2Q9 and D3Q27 are no exceptions. This would indicate that α will not be isotropic on these kinds of lattices even at lowest order in the Mach number. Let us for now suppose that we anyway have sixth order isotropy to proceed with the calculation. The sixth order isotropy conditions give us

$$\begin{aligned}K_{\theta\kappa\gamma\delta\varepsilon\zeta}\Pi_{\theta\kappa}^{(1)}\Pi_{\gamma\delta}^{(1)}\Pi_{\varepsilon\zeta}^{(1)}&=c_s^6[\Pi_{\theta\theta}^{(1)}(\Pi_{\kappa\kappa}^{(1)}\Pi_{\gamma\gamma}^{(1)}+6\Pi_{\kappa\gamma}\Pi_{\kappa\gamma})\\&\quad+8\Pi_{\theta\kappa}\Pi_{\kappa\gamma}\Pi_{\gamma\theta}].\end{aligned} \tag{21}$$

Therefore Eq. (20) becomes

$$\sum_{i=0}^{q-1}w_i(\boldsymbol{Q}_i{:}\boldsymbol{\Pi}^{(1)})^3=8c_s^6\Pi_{\theta\kappa}^{(1)}\Pi_{\kappa\gamma}^{(1)}\Pi_{\gamma\theta}^{(1)}. \tag{22}$$

Finally one finds for β

$$\beta=-\frac{2\Delta t}{3\rho c_s^2}\frac{\Pi_{\theta\kappa}^{(1)}\Pi_{\kappa\gamma}^{(1)}\Pi_{\gamma\theta}^{(1)}}{\Pi_{\lambda\mu}^{(1)}\Pi_{\lambda\mu}^{(1)}}. \tag{23}$$

Replacing this relation into Eq. (13) we obtain

$$\alpha=2-\frac{4\Delta t}{3\rho c_s^2}\frac{\Pi_{\theta\kappa}^{(1)}\Pi_{\kappa\gamma}^{(1)}\Pi_{\gamma\theta}^{(1)}}{\Pi_{\lambda\mu}^{(1)}\Pi_{\lambda\mu}^{(1)}}. \tag{24}$$

In order to obtain a result which is easier to understand physically we can replace $\boldsymbol{\Pi}^{(1)}$ by $\boldsymbol{S}$ using Eq. (17):

$$\alpha = 2 + \frac{4\Delta t}{3\omega_0 \alpha} \frac{S_{\theta\kappa} S_{\kappa\gamma} S_{\gamma\theta}}{S_{\lambda\mu} S_{\lambda\mu}}. \tag{25}$$

Multiplying on both sides by α and solving we get

$$\alpha = 1 + \sqrt{1 + \frac{4\Delta t}{3\omega_0} \frac{S_{\theta\kappa} S_{\kappa\gamma} S_{\gamma\theta}}{S_{\lambda\mu} S_{\lambda\mu}}} \cong 2 + \frac{2\Delta t}{3\omega_0} \frac{S_{\theta\kappa} S_{\kappa\gamma} S_{\gamma\theta}}{S_{\lambda\mu} S_{\lambda\mu}}, \tag{26}$$

where in the last equality we expanded the square root up to $O(\mathrm{Ma})$. Finally we use this last relation to evaluate $\beta = \alpha - 2$ and we can substitute β in Eq. (9),

$$\nu = \nu_0 - \frac{\Delta t c_s^2}{3\omega_0^2} \frac{S_{\theta\kappa} S_{\kappa\gamma} S_{\gamma\theta}}{S_{\lambda\mu} S_{\lambda\mu}}. \tag{27}$$

We see that the viscosity correction scales like $\|\boldsymbol{S}\|$ and this is similar to Smagorinsky's subgrid model [14] for turbulent viscosity $\nu = \nu_0 + \nu_t$ with

$$\nu_t = C_{\mathrm{smago}} \Delta x^2 (S_{\theta\kappa} S_{\theta\kappa})^{1/2}. \tag{28}$$

However, here, the viscosity corrections can be either positive or negative and present the ability to backscatter the energy. Finally the factor Δt indicates that in the limit of a fine lattice resolution ($\Delta t \to 0$) the correction to ν_0 vanishes, as expected for a subgrid model. There still remains an open question for us that would require further investigation. Is the subgrid model of Eq. (27) nothing else than an artifact of the ELBM, or is it a realistic representation of the unresolved physics? This question will be addressed in a future paper.

IV. NUMERICAL BENCHMARK

In this section we will validate the above analytical expressions for α by comparing numerical simulations performed with the various ways to compute it. For this purpose we will show that the ELBM goes to the LBGK as we refine the grid and that our approximation gives similar results with the exact ELBM solver. Finally we will contrast our results obtained with bounce-back, with the most accurate simulation we ran with more accurate boundary conditions (see below for more details). For the sake of the discussion, we need to introduce a name for the different entropic collision operators that we will compare.

The first approach uses a numerical method (Newton-Raphson algorithm) to compute α by solving Eq. (6). We name this approach NELBM for numerical entropic lattice Boltzmann model.

The second approach uses approximation Eq. (20) to compute α. We call it AELBM-NONISO for approximate entropic lattice Boltzmann with nonisotropic expression.

Finally, model AELBM-ISO gets α from approximation (24) and assumes an isotropic sixth order tensor.

A. Dipole-wall interaction test case

We now compare the NELBM, AELBM-NONISO, and AELBM-ISO on the so-called dipole-wall interaction benchmark. It is based on Ref. [8] and describes the case of a self-propelled dipole in a square box $\Gamma = [-1,1] \times [-1,1]$. The initial condition is given by two counter-rotating monopoles. The first one, located at $(x_1, y_1) = (0, 0.1)$ has positive core vorticity and the second one, located at $(x_2, y_2) = (0, -0.1)$ has negative core vorticity. The initial velocity field (u_x, u_y) is given by

$$u_x = -\frac{1}{2}\|\eta_e\|(y - y_1)\exp[-(r_1/r_0)^2] + \frac{1}{2}\|\eta_e\|(y - y_2)\exp[-(r_2/r_0)^2] \tag{29}$$

and

$$u_y = +\frac{1}{2}\|\eta_e\|(x - x_1)\exp[-(r_1/r_0)^2] - \frac{1}{2}\|\eta_e\|(x - x_2)\exp[-(r_2/r_0)^2], \tag{30}$$

where $r_i^2 = (x - x_i)^2 + (y - y_i)^2$, $i = 1, 2$, $r_0 = 0.1$ is the monopole diameter, and $\|\eta_e\| = 299.528\,385\,375\,226$ its core vorticity. This dipole has a net momentum directed towards the right wall in the x direction. At some point it will hit the wall and this will be the origin of turbulent dynamics and therefore of fast velocity variations. Since the analytical solution of α scales like the shear rate, this benchmark is well-suited to test our evaluation of α.

During the collision between the dipole and the wall, we observe a peak of mean enstrophy, computed as

$$\Omega(t) = \frac{1}{2}\int_{-1}^{1}\int_{-1}^{1} \eta^2(\boldsymbol{x}, t) d^2\boldsymbol{x}, \tag{31}$$

where $\eta = \partial_x u_y - \partial_y u_x$ is the vorticity. This value will be compared to $\Omega_{\mathrm{peak}} = 933.6$, which was found in [8] using a pseudospectral code, to gather information about the accuracy of our development in terms of the overall flow dynamics.

For this benchmark we use a Reynolds number of $\mathrm{Re} = 625$ and initialize our problem the following way. First we solve a Poisson equation

$$\nabla^2 p(\boldsymbol{x}) = -\boldsymbol{\nabla} \cdot ([\boldsymbol{u} \cdot \boldsymbol{\nabla}]\boldsymbol{u}), \quad \boldsymbol{x} \in \Gamma, \tag{32}$$

$$\frac{\partial p(\boldsymbol{x})}{\partial \boldsymbol{n}} = 0, \quad \boldsymbol{x} \in \partial\Gamma \tag{33}$$

using a second order finite difference scheme to get the correct initial pressure. Then we initialize the f_i using the first order approximation of the CE expansion $f_i \cong f_i^{(eq)} + f_i^{(1)}$ [see Eq. (16)].

We also used six different resolutions: $N = 500$, 1000, 1500, 2000, 2500, and 3000 in each spatial dimension. In order to avoid Mach number errors (see [13]) the characteristic velocity of the flow is scaled like $u_{\max} = u_{\max\ \mathrm{ref}} N / N_{\mathrm{ref}}$. This scaling actually means that, when refining the grid, we keep $\Delta x^2 / \Delta t$ constant, which also means that ω_0 does not have to change to keep the viscosity constant. In our benchmarks we take the reference values to be $N_{\mathrm{ref}} = 500$ and $u_{\max\ \mathrm{ref}} = 0.01$.

The boundary conditions (BC) used are fullway bounce-back (BB) which are consistent with the entropic formulation

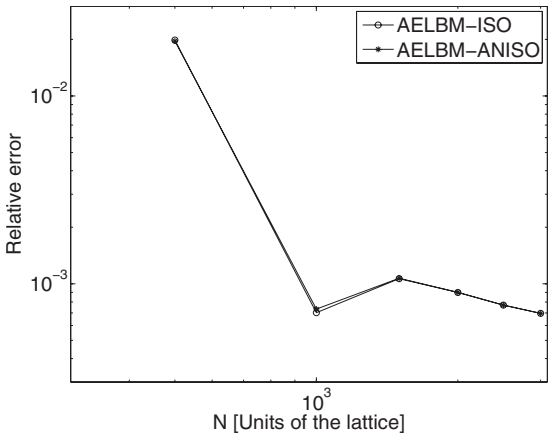

FIG. 2. Relative error on the enstrophy peak (with respect to [8]) as a function of space resolution, for the AELBM-ISO and AELBM-NONISO approximations.

since they do not allow an increase of the H function on the wall. In order to have second order accuracy in space, the actual location of the wall is in the middle of the last two lattice sites.

The dipole-wall interaction is simulated with three ways of calculating α until the physical time $t=0.371$ is reached. This time corresponds to the enstrophy peak $\Omega_{\text{peak}}=933.6$.

A first result is that AELBM-NONISO and AELBM-ISO models are very close. Figure 2 shows the relative error to Ω_{peak} as a function of the space resolution, for both the isotropic and nonisotropic ways of computing α. Due to the great similarity between the two models and for the sake of simplicity, we only keep the AELBM-ISO approximation until the end of this paper.

In Fig. 3 we compare the accuracy of NELBM, AELBM-ISO, as well as two LBGK models using, respectively, the BB and the regularized boundary (RB) conditions (see [4,15]). We see that the error is very similar for the NELBM and the AELBM-ISO, thus indicating that our analytical expression for α as a function of the strain rate tensor is meaningful.

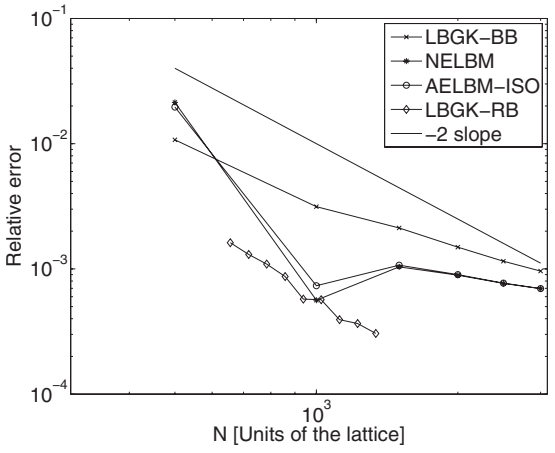

FIG. 3. Relative error on the enstrophy peak with respect to the resolution for the LBGK-BB (bounce-back BC), LBGK-RB (regularized BC), NELBM, and AELBM-ISO.

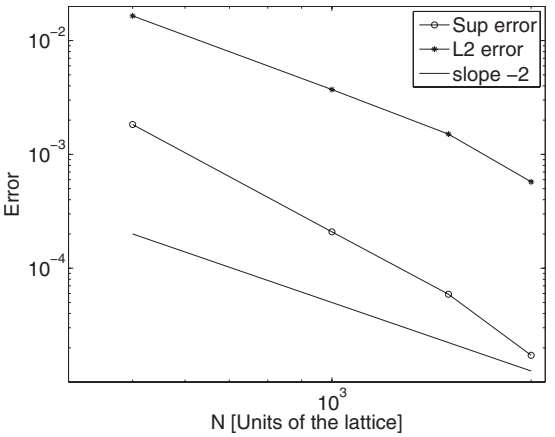

FIG. 4. Difference of the value of α as computed from Eq. (6) or Eq. (25).

At low resolution the difference between LBGK-BB and both ELBM codes is quite important. As the resolution increases the results become very close. We observe that the ELBM converges faster to the reference solution than the LBGK model with bounce-back.

We must also point out that the error for $N=1000$ is rather small for all ELBM. This result is due to the fact that for $N=500$ the enstrophy is way below Ω_{peak}. Then at $N \geqslant 1000$ the value of the peak becomes larger than Ω_{peak}, therefore at some point the numerical value computed with the ELBM crosses the Ω_{peak} value and actually this happens at about $N=1000$. Therefore the very good agreement of that point is rather a numerical accident than a feature of the model.

Finally we observe that the LBGK-RB model with the regularized boundary conditions outperforms all other approaches in terms of accuracy. Therefore the quality of boundary conditions seems to play a more important role on the precision of the simulation than the bulk dynamics.

These results suggest that ELBM (which uses bounce-back) is only marginally more accurate than LBGK-BB. Both seem to be equivalent when the spatial resolution is fine enough. Of course ELBM is always stable, even at an insufficient resolution; but in this case, it is far from clear whether the ELBM provides the correct physical behavior.

Finally, we study, in a quantitative way, the values of α as computed by NELBM and its approximation, AELBM. We consider two norms to evaluate the difference between the numerical and analytical α's. The sup and $\mathcal{L}^2$ errors are defined as

$$\|\alpha_{\text{NELBM}} - \alpha_{\text{AELBM}}\|_{\text{sup}} = \sup_{i,j} |\alpha_{\text{NELBM}}(i,j) - \alpha_{\text{AELBM}}(i,j)|, \tag{34}$$

$$\|\alpha_{\text{NELBM}} - \alpha_{\text{AELBM}}\|_{\mathcal{L}^2} = \sqrt{\sum_{i,j} [\alpha_{\text{NELBM}}(i,j) - \alpha_{\text{AELBM}}(i,j)]^2}, \tag{35}$$

where i,j are all the lattice nodes. The results are shown in Fig. 4. We observe that our analytical approximation of α in

terms of the strain rate tensor converges with about second accuracy in space to the numerical solution of Eq. (6). With $N=3000$ and a $\mathcal{L}^2$ norm of 10^{-2}, we see that the average difference between the two ways of calculating α is $10^{-2}/(3000)^2 \approx 10^{-9}$.

V. CONCLUSION

We showed, by giving an analytical evaluation of the viscosity correction, that the entropic lattice Boltzmann model can be interpreted as a subgrid model in the following sense: when the grid is under-resolved there is a correction to the viscosity which vanishes when increasing the resolution. We found that this correction goes to zero at the same rate as the time step Δt. When taking the limit of the lattice spacing $\Delta x \to 0$ while keeping the ratio $\Delta x^2/\Delta t$ constant, this means that the subgrid viscosity also scales as Δx^2, as in the standard Smagorinsky model.

Although the subgrid viscosity has a more complicated expression than Smagorinsky's one and can be positive or negative, it is, in magnitude, proportional to the strain rate. This subgrid correction was also found to be (slightly) anisotropic at $O(\mathrm{Ma})$ for the standard fourth-order isotropic lattices, such as D2Q9 or D3Q19.

From the benchmark we ran, we can nevertheless not conclude that this subgrid correction is physically sound or simply a numerical artifact to ensure numerical stability. Simulations of homogeneous turbulence conducted by Vahala [16] seem to indicate that ELBM and large eddy simulations such as the Smagorinsky model give identical results.

Finally we did not obtain an important gain in numerical accuracy for the bounce-back boundary condition between the LBGK and ELBM, and one can notice that using alternative boundary conditions, one can achieve results by one order of magnitude better. It is not clear, however, whether the regularized boundary condition is compatible with the ELBM scheme.

ACKNOWLEDGMENTS

We would like to thank Dr. J. Latt, Professor B. Boghosian, and Dr. A. Malaspinas for the enlightening discussions shared. O.M. also thankfully acknowledges the support of the Swiss National Science Foundation SNF (Grant No. FN 200021-107921).

[1] S. Succi, *The Lattice Boltzmann Equation for Fluid Dynamics and Beyond* (Oxford University Press, New York, 2001).
[2] P. L. Bhatnagar, E. P. Gross, and M. Krook, Phys. Rev. **94**, 511 (1954).
[3] D. d Humières, I. Ginzburg, M. Krafczyk, P. Lallemand, and L.-S. Luo, Philos. Trans. R. Soc. London, Ser. A **360**, 437 (2002).
[4] J. Latt and B. Chopard, Math. Comput. Simul. **72**, 165 (2006).
[5] S. Ansumali, S. Arcidiacono, S. S. Chikatamarla, N. I. Prasianakis, A. N. Gorban, and I. V. Karlin, Eur. Phys. J. B **56**, 135 (2007).
[6] S. Ansumali, Ph.D. dissertation, ETH Zürich, Zürich, Switzerland, 2004 (unpublished).
[7] S. Ansumali and I. V. Karlin, Phys. Rev. E **65**, 056312 (2002).
[8] H. J. H. Clercx and C.-H. Bruneau, Comput. Fluids **35**, 245 (2006).
[9] S. Ansumali, I. V. Karlin, and H. C. Öttinger, Europhys. Lett. **63**, 798 (2003).
[10] S. S. Chikatamarla, S. Ansumali, and I. V. Karlin, Phys. Rev. Lett. **97**, 010201 (2006).
[11] F. Tosi, S. Ubertini, S. Succi, and I. V. Karlin, J. Sci. Comput. **30**, 369 (2007).
[12] B. Chopard, A. Dupuis, A. Masselot, and P. Luthi, Adv. Complex Syst. **5**, 103 (2002).
[13] J. Latt, Ph.D. dissertation, University of Geneva, Geneva, Switzerland, 2007 (unpublished).
[14] J. Smagorinsky, Mon. Weather Rev. **91**, 99 (1963).
[15] J. Latt, B. Chopard, O. Malaspinas, M. Deville, and A. Michler, Phys. Rev. E **77**, 056703 (2008).
[16] M. Soe, B. Keatinf, G. Vahala, J. Yepez, and L. Vahala, *Large Eddy-Lattice Boltzmann Simulation and MHD Turbulence* (DSFD, Banff, 2007).